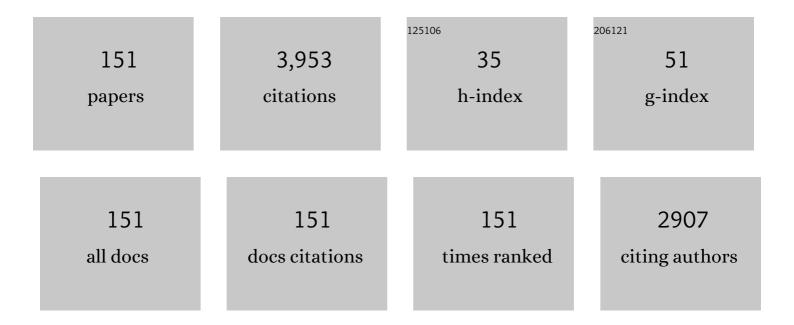
Aiying Wang

List of Publications by Year in descending order

Source: https://exaly.com/author-pdf/8588189/publications.pdf Version: 2024-02-01



#	Article	IF	CITATIONS
1	Insights on high temperature friction mechanism of multilayer ta-C films. Journal of Materials Science and Technology, 2022, 97, 29-37.	5.6	22
2	Phase orientation improved the corrosion resistance and conductivity of Cr2AlC coatings for metal bipolar plates. Journal of Materials Science and Technology, 2022, 105, 36-44.	5.6	25
3	Self-Supporting Ultrathin DLC/Si ₃ N ₄ /SiO ₂ for Micro-Pressure Sensor. IEEE Sensors Journal, 2022, 22, 3937-3944.	2.4	3
4	Sandwich-zigzag structure enhanced erosion resistance of TiN coatings. Materials Letters, 2022, 310, 131496.	1.3	4
5	Long-term tribocorrosion resistance and failure tolerance of multilayer carbon-based coatings. Friction, 2022, 10, 1707-1721.	3.4	7
6	Controlling the compactness and sp2 clusters to reduce interfacial damage of amorphous carbon/316L bipolar plates in PEMFCs. International Journal of Hydrogen Energy, 2022, 47, 11622-11632.	3.8	7
7	Controllable defect engineering to enhance the corrosion resistance of Cr/GLC multilayered coating for deep-sea applications. Corrosion Science, 2022, 199, 110175.	3.0	16
8	Accelerated deterioration mechanism of 316L stainless steel in NaCl solution under the intermittent tribocorrosion process. Journal of Materials Science and Technology, 2022, 121, 67-79.	5.6	13
9	Balancing the corrosion resistance and conductivity of Cr-Al-C coatings via annealing treatment for metal bipolar plates. Applied Surface Science, 2022, 597, 153670.	3.1	10
10	SiFBA5, a cold-responsive factor from Saussurea involucrata promotes cold resilience and biomass increase in transgenic tomato plants under cold stress. BMC Plant Biology, 2021, 21, 75.	1.6	14
11	Exploring the tribological behavior of Ti/Al-DLC/PAO/graphene oxide nanocomposite system. Ceramics International, 2021, 47, 11052-11062.	2.3	9
12	Insights into Superlow Friction and Instability of Hydrogenated Amorphous Carbon/Fluid Nanocomposite Interface. ACS Applied Materials & Interfaces, 2021, 13, 35173-35186.	4.0	17
13	Erosion behavior and failure mechanism of Ti/TiAlN multilayer coatings eroded by silica sand and glass beads. Journal of Materials Science and Technology, 2021, 80, 179-190.	5.6	39
14	Tribological mechanism of (Cr, V)N coating in the temperature range of 500–900°C. Tribology International, 2021, 159, 106952.	3.0	12
15	Cr/GLC multilayered coating in simulated deep-sea environment: Corrosion behavior and growth defect evolution. Corrosion Science, 2021, 188, 109528.	3.0	25
16	One-step plasma nitriding synthesis of NixN/NF (xÂ=Â3, 4) for efficient hydrogen evolution. Applied Surface Science, 2021, 561, 149972.	3.1	11
17	Corrosion mechanism of Ti2AlC MAX phase coatings under the synergistic effects of water vapor and solid NaCl at 600°C. Corrosion Science, 2021, 192, 109788.	3.0	25
18	Diamond-like carbon based micro-pressure sensor with ultra-thin sensitive membrane. , 2021, , .		1

#	Article	IF	CITATIONS
19	Adhesion, biological corrosion resistance and biotribological properties of carbon films deposited on MAO coated Ti substrates. Journal of the Mechanical Behavior of Biomedical Materials, 2020, 101, 103448.	1.5	27
20	Reducing the self-healing temperature of Ti2AlC MAX phase coating by substituting Al with Sn. Journal of the European Ceramic Society, 2020, 40, 197-201.	2.8	23
21	Diffusion-controlled intercalation approach to synthesize the Ti2AlC MAX phase coatings at low temperature of 550†°C. Applied Surface Science, 2020, 502, 144130.	3.1	17
22	Influence of deposition temperature on the structure, optical and electrical properties of a-C films by DCMS. Applied Surface Science, 2020, 503, 144310.	3.1	12
23	Crystalline transformation from ta-C to graphene induced by a catalytic Ni layer during annealing. Diamond and Related Materials, 2020, 101, 107556.	1.8	5
24	MEMS piezo-resistive force sensor based on DC sputtering deposited amorphous carbon films. Sensors and Actuators A: Physical, 2020, 303, 111700.	2.0	14
25	Transforming the amorphous Ti-Al-C coatings to high-purity Ti2AlC MAX phase coatings by prolonged annealing at 550°C. Materials Letters, 2020, 261, 127160.	1.3	15
26	Corrosion behavior of diamond-like carbon film induced by Al/Ti co-doping. Applied Surface Science, 2020, 509, 144877.	3.1	29
27	Spectroscopic investigation on the near-substrate plasma characteristics of chromium HiPIMS in low density discharge mode. Plasma Sources Science and Technology, 2020, 29, 015013.	1.3	12
28	Three-dimensional hierarchical mesoporous carbon for regenerative electrochemical dopamine sensor. Electrochimica Acta, 2020, 360, 137016.	2.6	43
29	Amorphous carbon to graphene: Carbon diffusion via nickel catalyst. Materials Letters, 2020, 278, 128468.	1.3	3
30	Structural and mechanism study on enhanced thermal stability of hydrogenated diamond-like carbon films doped with Si/O. Diamond and Related Materials, 2020, 108, 107923.	1.8	16
31	Understanding the effect of Al/Ti ratio on the tribocorrosion performance of Al/Ti co-doped diamond-like carbon films for marine applications. Surface and Coatings Technology, 2020, 402, 126347.	2.2	17
32	Fundamental understanding on low-friction mechanisms at amorphous carbon interface from reactive molecular dynamics simulation. Carbon, 2020, 170, 621-629.	5.4	23
33	Residual Compressive Stress Enabled 2D-to-3D Junction Transformation in Amorphous Carbon Films for Stretchable Strain Sensors. ACS Applied Materials & Interfaces, 2020, 12, 45549-45557.	4.0	11
34	Protective Geopolymer Coatings Containing Multi-Componential Precursors: Preparation and Basic Properties Characterization. Materials, 2020, 13, 3448.	1.3	10
35	Role of dimple textured surface on tribological properties of Ti/Al-codoped diamond-like carbon films. Thin Solid Films, 2020, 708, 138136.	0.8	8
36	Anti-wear Cr-V-N coating via V solid solution: Microstructure, mechanical and tribological properties. Surface and Coatings Technology, 2020, 397, 126048.	2.2	14

#	Article	IF	CITATIONS
37	Interface-induced degradation of amorphous carbon films/stainless steel bipolar plates in proton exchange membrane fuel cells. Journal of Power Sources, 2020, 469, 228269.	4.0	32
38	Cooling rate dependence of Ni-catalyzed transformation of amorphous carbon into graphene in rapid thermal processing: An experimental and reactive molecular dynamics study. Applied Surface Science, 2020, 529, 147042.	3.1	2
39	High-performance Cr2AlC MAX phase coatings: Oxidation mechanisms in the 900–1100°C temperature range. Corrosion Science, 2020, 167, 108492.	3.0	43
40	Corrosion resistance of amorphous carbon film in 3.5Âwt% NaCl solution for marine application. Electrochimica Acta, 2020, 346, 136282.	2.6	31
41	Tailored electrochemical behavior of ta-C film by glancing angle deposition. Applied Surface Science, 2020, 516, 146115.	3.1	9
42	Comparative study on protective properties of CrN coatings on the ABS substrate by DCMS and HiPIMS techniques. Surface and Coatings Technology, 2020, 394, 125890.	2.2	29
43	Fast Synthesis of Graphene with a Desired Structure via Ni-Catalyzed Transformation of Amorphous Carbon during Rapid Thermal Processing: Insights from Molecular Dynamics and Experimental Study. Journal of Physical Chemistry C, 2019, 123, 27834-27842.	1.5	4
44	Piezoresistive behavior of amorphous carbon films for high performance MEMS force sensors. Applied Physics Letters, 2019, 114, .	1.5	16
45	Microstructure and property evolution of diamond-like carbon films co-doped by Al and Ti with different ratios. Surface and Coatings Technology, 2019, 361, 83-90.	2.2	31
46	Transformation of amorphous carbon to graphene on low-index Ni surfaces during rapid thermal processing: a reactive molecular dynamics study. Physical Chemistry Chemical Physics, 2019, 21, 2271-2275.	1.3	8
47	Enhanced tribological and corrosion properties of multilayer ta-C films via alternating sp3 content. Surface and Coatings Technology, 2019, 374, 317-326.	2.2	36
48	Insights into friction dependence of carbon nanoparticles as oil-based lubricant additive at amorphous carbon interface. Carbon, 2019, 150, 465-474.	5.4	48
49	Role of deposition temperature on the mechanical and tribological properties of Cu and Cr co-doped diamond-like carbon films. Thin Solid Films, 2019, 678, 16-25.	0.8	22
50	A high oxidation resistance Ti2AlC coating on Zirlo substrates for loss-of-coolant accident conditions. Ceramics International, 2019, 45, 13912-13922.	2.3	46
51	Atomistic understanding on friction behavior of amorphous carbon films induced by surface hydrogenated modification. Tribology International, 2019, 136, 446-454.	3.0	26
52	Role of the carbon source in the transformation of amorphous carbon to graphene during rapid thermal processing. Physical Chemistry Chemical Physics, 2019, 21, 9384-9390.	1.3	12
53	Movement of luminous group spots on target and size modification of micro-particles during cathodic vacuum arc deposition. Vacuum, 2019, 164, 381-389.	1.6	5
54	Comparative study on oxidation behavior of Ti2AlN coatings in air and pure steam. Ceramics International, 2019, 45, 9260-9270.	2.3	9

#	Article	IF	CITATIONS
55	Bactericidal abilities and in vitro properties of diamond-like carbon films deposited onto MAO-treated titanium. Materials Letters, 2019, 244, 155-158.	1.3	10
56	Role of unsaturated hydrocarbon lubricant on the friction behavior of amorphous carbon films from reactive molecular dynamics study. Computational Materials Science, 2019, 161, 1-9.	1.4	18
57	Micro Pressure Sensors Based on Ultra-thin Amorphous Carbon Film as both Sensitive and Structural Components. , 2019, , .		1
58	Enhanced mechanical and tribological properties of V-Al-C coatings via increasing columnar boundaries. Journal of Alloys and Compounds, 2019, 781, 186-195.	2.8	16
59	Insights on low-friction mechanism of amorphous carbon films from reactive molecular dynamics study. Tribology International, 2019, 131, 567-578.	3.0	41
60	Tribological properties of Tiâ€doped diamondâ€like carbon coatings under dry friction and PAO oil lubrication. Surface and Interface Analysis, 2019, 51, 361-370.	0.8	22
61	Gas Breakdown and Discharge Formation in High-Power Impulse Magnetron Sputtering. IEEE Transactions on Plasma Science, 2019, 47, 1215-1222.	0.6	6
62	Dense nanocolumnar structure induced anti-corrosion CrB2 coating with (0â€ [−] 0â€ [−] 1) preferred orientation deposited by DC magnetron sputtering. Materials Letters, 2019, 240, 180-184.	1.3	14
63	Triboâ€Induced Structural Transformation and Lubricant Dissociation at Amorphous Carbon–Alpha Olefin Interface. Advanced Theory and Simulations, 2019, 2, 1800157.	1.3	18
64	Tribological mechanism of diamond-like carbon films induced by Ti/Al co-doping. Surface and Coatings Technology, 2018, 342, 167-177.	2.2	33
65	Fabrication and mechanical properties of high purity of Cr2AlC coatings by adjustable Al contents. Journal of Alloys and Compounds, 2018, 753, 11-17.	2.8	20
66	The influence of superimposed DC current on electrical and spectroscopic characteristics of HiPIMS discharge. AIP Advances, 2018, 8, .	0.6	7
67	Structural design of Cr/GLC films for high tribological performance in artificial seawater: Cr/GLC ratio and multilayer structure. Journal of Materials Science and Technology, 2018, 34, 1273-1280.	5.6	31
68	Enhanced Tribocorrosion Performance of Cr/GLC Multilayered Films for Marine Protective Application. ACS Applied Materials & amp; Interfaces, 2018, 10, 13187-13198.	4.0	70
69	Bulk-limited electrical behaviors in metal/hydrogenated diamond-like carbon/metal devices. Applied Physics Letters, 2018, 112, .	1.5	8
70	Enhancing slurryabilities of five lignites from Inner Mongolia of China by microwave irradiation. Drying Technology, 2018, 36, 100-108.	1.7	8
71	A Hierarchically Porous Carbon Fabric for Highly Sensitive Electrochemical Sensors. Advanced Engineering Materials, 2018, 20, 1700608.	1.6	18
72	Mechanism of contact pressure-induced friction at the amorphous carbon/alpha olefin interface. Npj Computational Materials, 2018, 4, .	3.5	44

#	Article	IF	CITATIONS
73	Comparison of empirical potentials for calculating structural properties of amorphous carbon films by molecular dynamics simulation. Computational Materials Science, 2018, 151, 246-254.	1.4	38
74	Metal Buffer Layer on Structure, Mechanical and Tribological Property of GLC films. Wuji Cailiao Xuebao/Journal of Inorganic Materials, 2018, 33, 331.	0.6	3
75	Microstructure and mechanical properties of Ti/Al co-doped DLC films: Dependence on sputtering current, source gas, and substrate bias. Applied Surface Science, 2017, 410, 51-59.	3.1	51
76	Friction and Wear Mechanism of MoS2/C Composite Coatings Under Atmospheric Environment. Tribology Letters, 2017, 65, 1.	1.2	28
77	Temperature induced superhard CrB 2 coatings with preferred (001) orientation deposited by DC magnetron sputtering technique. Surface and Coatings Technology, 2017, 322, 134-140.	2.2	19
78	Dense and high-stability Ti2AlN MAX phase coatings prepared by the combined cathodic arc/sputter technique. Applied Surface Science, 2017, 396, 1435-1442.	3.1	45
79	Discharge state transition and cathode fall thickness evolution during chromium HiPIMS discharge. Physics of Plasmas, 2017, 24, .	0.7	9
80	Stress reduction mechanism of diamond-like carbon films incorporated with different Cu contents. Thin Solid Films, 2017, 640, 45-51.	0.8	28
81	Ab Initio Study of Interfacial Structure Transformation of Amorphous Carbon Catalyzed by Ti, Cr, and W Transition Layers. ACS Applied Materials & Interfaces, 2017, 9, 41115-41119.	4.0	19
82	The effect of substrate bias on the characteristics of CrN coatings deposited by DC-superimposed HiPIMS system. International Journal of Modern Physics B, 2017, 31, 1744032.	1.0	4
83	Comparative study on structure and wetting properties of diamond-like carbon films by W and Cu doping. Diamond and Related Materials, 2017, 73, 278-284.	1.8	27
84	Ti/Al co-doping induced residual stress reduction and bond structure evolution of amorphous carbon films: An experimental and ab initio study. Carbon, 2017, 111, 467-475.	5.4	39
85	De Novo Transcriptome Sequencing and the Hypothetical Cold Response Mode of Saussurea involucrata in Extreme Cold Environments. International Journal of Molecular Sciences, 2017, 18, 1155.	1.8	20
86	Synergistic effect of Cu/Cr co-doping on the wettability and mechanical properties of diamond-like carbon films. Diamond and Related Materials, 2016, 68, 1-9.	1.8	43
87	Developing transparent copper-doped diamond-like carbon films for marine antifouling applications. Diamond and Related Materials, 2016, 69, 144-151.	1.8	38
88	Hard yet tough V-Al-C-N nanocomposite coatings: Microstructure, mechanical and tribological properties. Surface and Coatings Technology, 2016, 304, 553-559.	2.2	16
89	Stress measurement at the interface between a Si substrate and diamond-like carbon/Cr/W films by the electronic backscatter diffraction method. Applied Physics Express, 2016, 9, 025504.	1.1	1
90	Effect of metal doping on structural characteristics of amorphous carbon system: A first-principles study. Thin Solid Films, 2016, 607, 67-72.	0.8	20

#	Article	IF	CITATIONS
91	Microstructure evolution of V–Al–C coatings synthesized from a V 2 AlC compound target after vacuum annealing treatment. Journal of Alloys and Compounds, 2016, 661, 476-482.	2.8	27
92	Structure and residual stress evolution of Ti/Al, Cr/Al or W/Al co-doped amorphous carbon nanocomposite films: Insights from ab initio calculations. Materials and Design, 2016, 89, 1123-1129.	3.3	23
93	Physicochemical characterizations for improving the slurryability of Philippine lignite upgraded through microwave irradiation. RSC Advances, 2015, 5, 14690-14696.	1.7	20
94	Nanostructured Carbon Materials. Journal of Nanomaterials, 2015, 2015, 1-2.	1.5	4
95	Ab Initio Investigation on Cu/Cr Codoped Amorphous Carbon Nanocomposite Films with Giant Residual Stress Reduction. ACS Applied Materials & Interfaces, 2015, 7, 27878-27884.	4.0	38
96	Characterization and properties of duplex a-C:H/MAO coatings on magnesium alloy using combined microarc oxidation and hybrid magnetron sputtering. Journal Wuhan University of Technology, Materials Science Edition, 2015, 30, 822-826.	0.4	4
97	Amorphous self-lubricant MoS2-C sputtered coating with high hardness. Applied Surface Science, 2015, 331, 66-71.	3.1	72
98	Structural properties and surface wettability of Cu-containing diamond-like carbon films prepared by a hybrid linear ion beam deposition technique. Thin Solid Films, 2015, 584, 289-293.	0.8	30
99	Microstructure and electrochemical properties of nitrogen-doped DLC films deposited by PECVD technique. Applied Surface Science, 2015, 329, 281-286.	3.1	61
100	Probing the Stress Reduction Mechanism of Diamond-Like Carbon Films by Incorporating Ti, Cr, or W Carbide-Forming Metals: Ab Initio Molecular Dynamics Simulation. Journal of Physical Chemistry C, 2015, 119, 6086-6093.	1.5	33
101	Upgrading Chinese Shengli lignite by microwave irradiation for slurribility improvement. Fuel, 2015, 159, 909-916.	3.4	26
102	The scaling behavior and mechanism of Ti2AlC MAX phase coatings in air and pure water vapor. Surface and Coatings Technology, 2015, 272, 380-386.	2.2	18
103	Microstructure and mechanical property of diamond-like carbon films with ductile copper incorporation. Surface and Coatings Technology, 2015, 272, 33-38.	2.2	40
104	Preparation of Ti2AlC MAX Phase Coating by DC Magnetron Sputtering Deposition and Vacuum Heat Treatment. Journal of Materials Science and Technology, 2015, 31, 1193-1197.	5.6	36
105	Stress reduction of Cu-doped diamond-like carbon films from ab initio calculations. AIP Advances, 2015, 5, .	0.6	9
106	Microstructure and properties of (Cr:N)-DLC films deposited by a hybrid beam technique. Surface and Coatings Technology, 2015, 261, 398-403.	2.2	22
107	Ab initio molecular dynamics simulation on stress reduction mechanism of Ti-doped diamond-like carbon films. Thin Solid Films, 2015, 584, 204-207.	0.8	10
108	Influence of Substrate Negative Bias on Structure and Properties of TiN Coatings Prepared by Hybrid HIPIMS Method. Journal of Materials Science and Technology, 2015, 31, 37-42.	5.6	59

#	Article	IF	CITATIONS
109	Functional Carbon Nanomaterials. Journal of Nanomaterials, 2014, 2014, 1-2.	1.5	1
110	Stress reduction dependent on incident angles of carbon ions in ultrathin tetrahedral amorphous carbon films. Applied Physics Letters, 2014, 104, 141908.	1.5	9
111	Molecular dynamics simulation for the influence of incident angles of energetic carbon atoms on the structure and properties of diamond-like carbon films. Thin Solid Films, 2014, 552, 136-140.	0.8	27
112	Cloning and characterization of a novel dehydrin gene, SiDhn2, from Saussurea involucrata Kar. et Kir Plant Molecular Biology, 2014, 84, 707-718.	2.0	37
113	Thickness dependence of properties and structure of ultrathin tetrahedral amorphous carbon films: A molecular dynamics simulation. Surface and Coatings Technology, 2014, 258, 938-942.	2.2	8
114	Amperometric glucose sensor based on boron doped microcrystalline diamond film electrode with different boron doping levels. RSC Advances, 2014, 4, 58349-58356.	1.7	22
115	Membrane Damage Induced by Supercritical Carbon Dioxide in Rhodotorula mucilaginosa. Indian Journal of Microbiology, 2013, 53, 352-358.	1.5	13
116	Influence of bias voltage on microstructure and properties of Al-containing diamond-like carbon films deposited by a hybrid ion beam system. Surface and Coatings Technology, 2013, 229, 217-221.	2.2	25
117	Microstructure, mechanical and tribological behaviors of MoS2-Ti composite coatings deposited by a hybrid HIPIMS method. Surface and Coatings Technology, 2013, 228, 275-281.	2.2	89
118	Stress reduction of diamond-like carbon by Si incorporation: A molecular dynamics study. Surface and Coatings Technology, 2013, 228, S190-S193.	2.2	22
119	Microstructure and properties of duplex (Ti:N)-DLC/MAO coating on magnesium alloy. Applied Surface Science, 2013, 270, 519-525.	3.1	29
120	Structural properties and growth evolution of diamond-like carbon films with different incident energies: A molecular dynamics study. Applied Surface Science, 2013, 273, 670-675.	3.1	63
121	Graphite-like carbon films by high power impulse magnetron sputtering. Applied Surface Science, 2013, 283, 321-326.	3.1	67
122	Microstructure and tribological behavior of self-lubricating (Si:N)-DLC/MAO coatings on AZ80 magnesium substrate. Acta Metallurgica Sinica (English Letters), 2013, 26, 693-698.	1.5	14
123	Growth properties and resistive switching effects of diamond-like carbon films deposited using a linear ion source. Journal of Vacuum Science and Technology B:Nanotechnology and Microelectronics, 2013, 31, .	0.6	6
124	Incorporated W Roles on Microstructure and Properties of W-C:H Films by a Hybrid Linear Ion Beam Systems. Journal of Nanomaterials, 2013, 2013, 1-8.	1.5	6
125	Chemical Bond Structure of Metal-Incorporated Carbon System. Journal of Computational and Theoretical Nanoscience, 2013, 10, 1688-1692.	0.4	7
126	Corrosion resistance of composite coating on magnesium alloy using combined microarc oxidation and inorganic sealing. Transactions of Nonferrous Metals Society of China, 2012, 22, s760-s763.	1.7	15

#	Article	IF	CITATIONS
127	Effect of Negatively Charged lons on the Formation of Microarc Oxidation Coating on 2024 Aluminium Alloy. Journal of Materials Science and Technology, 2012, 28, 707-712.	5.6	21
128	Effect of substrate bias on microstructure and tribological performance of GLC films using hybrid HIPIMS technique. Transactions of Nonferrous Metals Society of China, 2012, 22, s740-s744.	1.7	6
129	Investigation of the microstructure, mechanical properties and tribological behaviors of Ti-containing diamond-like carbon films fabricated by a hybrid ion beam method. Thin Solid Films, 2012, 520, 6057-6063.	0.8	56
130	First principles investigation of interaction between impurity atom (Si, Ge, Sn) and carbon atom in diamond-like carbon system. Thin Solid Films, 2012, 520, 6064-6067.	0.8	3
131	Deposition and properties of Al-containing diamond-like carbon films by a hybrid ion beam sources. Journal of Alloys and Compounds, 2011, 509, 4626-4631.	2.8	94
132	Synthesis, characterization and properties of the DLC films with low Cr concentration doping by a hybrid linear ion beam system. Surface and Coatings Technology, 2011, 205, 2882-2886.	2.2	45
133	Microstructure and property evolution of Cr-DLC films with different Cr content deposited by a hybrid beam technique. Vacuum, 2011, 85, 792-797.	1.6	83
134	Discovery of 6-(Aminomethyl)-5-(2,4-dichlorophenyl)-7-methylimidazo[1,2- <i>a</i>]pyrimidine-2-carboxamides as Potent, Selective Dipeptidyl Peptidase-4 (DPP4) Inhibitors. Journal of Medicinal Chemistry, 2010, 53, 5620-5628.	2.9	41
135	Surface microstructurization of a sputtered magnesium thin film via a solution–immersion route. Materials Letters, 2010, 64, 475-478.	1.3	13
136	Influence of interlayers on corrosion resistance of diamond-like carbon coating on magnesium alloy. Surface and Coatings Technology, 2010, 204, 2193-2196.	2.2	65
137	Improving wear resistance and corrosion resistance of AZ31 magnesium alloy by DLC/AlN/Al coating. Surface and Coatings Technology, 2010, 205, 2067-2073.	2.2	85
138	Effect of bias voltage on growth property of Cr-DLC film prepared by linear ion beam deposition technique. Vacuum, 2010, 85, 231-235.	1.6	94
139	Structure and elastic recovery of Cr–C:H films deposited by a reactive magnetron sputtering technique. Applied Surface Science, 2010, 257, 244-248.	3.1	22
140	Synthesis and SAR of azolopyrimidines as potent and selective dipeptidyl peptidase-4 (DPP4) inhibitors for type 2 diabetes. Bioorganic and Medicinal Chemistry Letters, 2010, 20, 4395-4398.	1.0	47
141	Synthesis, SAR, and atropisomerism of imidazolopyrimidine DPP4 inhibitors. Bioorganic and Medicinal Chemistry Letters, 2010, 20, 6273-6276.	1.0	18
142	Nonvolatile resistive switching memory based on amorphous carbon. Applied Physics Letters, 2010, 96,	1.5	133
143	Preparation, characterization and properties of Cr-incorporated DLC films on magnesium alloy. Diamond and Related Materials, 2010, 19, 1307-1315.	1.8	89
144	Fabrication of Cr coating on AZ31 magnesium alloy by magnetron sputtering. Transactions of Nonferrous Metals Society of China, 2008, 18, s329-s333.	1.7	18

#	Article	IF	CITATIONS
145	Structure and mechanical properties of W incorporated diamond-like carbon films prepared by a hybrid ion beam deposition technique. Carbon, 2006, 44, 1826-1832.	5.4	161
146	Unusual stress behavior in W-incorporated hydrogenated amorphous carbon films. Applied Physics Letters, 2005, 86, 111902.	1.5	42
147	Effect of Substrate Bias on Structure and Properties of W incorporated Diamond-like Carbon Films. Materials Research Society Symposia Proceedings, 2004, 821, 7.	0.1	0
148	Two-dimensional simulations of temperature fields of the reactor wall during hot-filament CVD diamond film growth over a large area. Modelling and Simulation in Materials Science and Engineering, 2004, 12, 325-335.	0.8	4
149	Properties of transparent conducting ZnO : Al oxide thin films and their application for molecular organic light-emitting diodes. Journal of Materials Science: Materials in Electronics, 2004, 15, 169-174.	1.1	19
150	Influence of quantity and energy of the particles in gas phase on nucleation of the HFCVD of diamond films. Materials Letters, 2001, 48, 8-14.	1.3	1
151	Influence of Nitrogen Partial Pressure on the Microstructure and Properties of TiN Coatings. Advanced Materials Research, 0, 1049-1050, 89-93.	0.3	Ο